

## Quantum-electromagnetic excitations in bismuth

M. Giura, R. Marcon, and P. Marietti

*Istituto di Fisica, Facoltà di Ingegneria, Università di Roma, Roma, Italy*  
*and Gruppo Nazionale di Struttura della Materia del Consiglio Nazionale delle Ricerche, Roma, Italy*

(Received 3 April 1979; revised manuscript received 20 September 1979)

We have observed quantum-electromagnetic waves in pure bismuth samples. The quantum nature of these waves follows from the following: (1) the oscillating behavior of the microwave absorption versus magnetic field  $H$  displays  $\Delta(1/H)$  periods related to the extremal cross-sectional areas of the Fermi surface, (2) for  $\vec{H}$  nearly orthogonal to the wave vector  $\vec{q}$ , the amplitude of the oscillations diminishes and the periods are related to the nonextremal areas. The peculiar physical aspects of this phenomenon are that the cross-sectional areas are the largest ones in bismuth and that resonances are missing below a certain value of the Landau quantum number.

### I. INTRODUCTION

An oscillating behavior of the microwave surface impedance, as a function of the magnetic field  $H$ , is to be expected in each metal for which de Haas-van Alphen or quantum ultrasound oscillations have been observed, because the transport phenomena are affected by the energy-level quantization in a magnetic field. So far, however, no experimental evidence exists of this effect, notwithstanding the large number of electromagnetic excitations that are possible and have been detected in metals. A good review of the subject can be found in a paper by Kaner and Skobov.<sup>1</sup>

In the infrared range, resonances were found in bismuth, under the condition  $\hbar\omega > \epsilon_F$  (where  $\epsilon_F$  is the Fermi energy), owing to both inter<sup>2</sup> and intra-band<sup>3</sup> transitions between Landau levels. In the microwave range (10–100 GHz) the most important effect is cyclotron resonance which is a classic effect ( $\hbar\omega < k_B T < \epsilon_F$  at helium temperature), while the sole quantum effect observed by many authors<sup>4–7</sup> consists in a modulation of the Alfvén-wave analog to the Shubnikov–de Haas effect for the resistivity. Its physical origin lies in the energy dependence of the relaxation time  $\tau$  and affects the Alfvén-wave damping.

At any rate, no one has observed resonances due to Landau levels crossing the Fermi level in the collisionless-damping regime except Spong and Kip<sup>8</sup> who measured an oscillating microwave absorption of the de Haas–van Alphen type in aluminum. The analysis of these authors is devoted to finding the correlation between surface impedance and susceptibility measurements: They point out that the two methods are complementary. Demikhovskii and Protogenov<sup>9</sup> in a recent theoretical paper have stressed the prominence of quantum-electromagnetic waves for metals and semimetals with different carrier dispersion laws. They conclude by bringing to the attention of experimental-

ists these, at that time unobserved, quantum-electromagnetic excitations.

In a previous paper<sup>10</sup> we presented a set of measurements showing an absorption thought to be of the de Haas–van Alphen type. In this paper a complete set of measurements is presented which shows that the found microwave absorption is similar to the quantum giant oscillations of ultrasound absorption. That is to say, it is explicable in terms of energy and momentum conservation when a photon is absorbed by an electron whose Landau energy level crosses the Fermi level.

This statement is based on the fact that the periods  $\Delta(1/H)$  of the oscillations are related to the extremal cross-sectional areas of the Fermi surface when  $\vec{H}$  is far from orthogonality with respect to the microwave wave vector  $\vec{q}$ , while, as  $\vec{H}$  becomes near orthogonal to  $\vec{q}$ , nonextremal cross sections are measured. Moreover, these oscillations are present when the size of the samples along  $\vec{q}$  is larger than  $\sim 0.5$  cm and resonances are missing below a certain value of the Landau quantum number.

In Sec. II the experimental setup is sketched; in Sec. III the measurements are presented; in Sec. IV the experimental details are discussed; and in Sec. V the conclusions are presented.

### II. EXPERIMENTAL SETUP

The microwave-absorption measurements were carried out by means of a standard microwave technique at frequencies between 22 and 24 GHz. Variations of the sample surface impedance as a function of the static magnetic field  $H$  were observed by detecting the change in the  $Q$  factor of a rectangular reflection cavity operating in the  $H_{011}$  mode. The sample was positioned so as to be one of the cavity side walls. The resonant cavity was in contact with liquid helium at  $T = 1.3$  K. The microwave power from a Gunn generator was fre-

quency controlled by a Pound stabilizer. The low-frequency signal, derived from a heterodyne detector, was fed into a lock-in amplifier synchronized with the static-magnetic-field modulation. The lock-in output was recorded on a XY plotter. The direction of  $\vec{H}$  could be rotated in a horizontal plane by so allowing the angle  $\theta$  between  $\vec{H}$  and the normal to the sample surface to vary.

Ultrasounds were sent on the samples by means of a pulse technique, and all was arranged in order to carry out ultrasound-absorption measurements simultaneously with microwave ones. The ultrasound frequency was 70 MHz. The setup has been described in detail in a previous paper.<sup>11</sup> Single crystals of pure Bi (99.9999%) of size  $l \times 1.0 \times 1.2$  cm<sup>3</sup> were used. The size  $l$  was varied between 0.55 and 0.45 cm.

### III. EXPERIMENTAL RESULTS

In this section we present experimental results concerning a new type of oscillations of the microwave magnetic absorption which are undoubtedly related to the energy-level quantization induced by a magnetic field: We are then in the presence of quantum-electromagnetic oscillations (QEO). In other words these are the analog, with respect to microwaves, of the giant quantum oscillations in ultrasound absorption.

Since it is the first time that this phenomenon has been clearly observed, a wide set of measurements has been carried out in order to understand its physical origin. This is the reason why we put much emphasis on the description of the experimental results. These are summarized as follows.

(i) A typical oscillation pattern of the derivative  $dR/dH$  of the surface impedance of the Bi sample vs  $H$  is presented in Fig. 1. The oscillations are periodic as a function of  $1/H$  and the period does not depend on the microwave frequency in our measurement range (22–24 GHz). In Fig. 2 the values ( $1/H$ ) of the reciprocal of the field for which  $dR/dH$  presents a minimum are plotted vs the resonance-order number  $n$ .

The periods  $\Delta(1/H)$  are directly related to the areas  $S_F$  of extremal cross sections of the Fermi surface. To show this we have measured  $\Delta(1/H)$

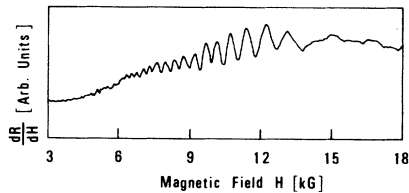


FIG. 1. Typical  $dR/dH$  vs  $H$  measurement for  $\vec{H}$  directed along the binary axis.

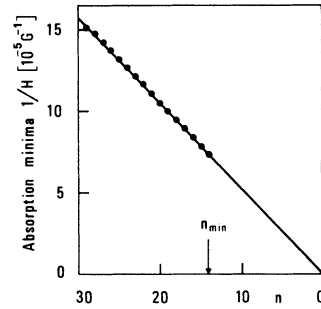


FIG. 2. Absorption minima  $1/H$  vs the order number  $n$  of oscillations in Fig. 1.

with  $\vec{H}$  lying in the binary-bisector plane for sample N.1 (Fig. 3) and in the bisector-trigonal plane for sample N.2 (Fig. 4). In these figures the experimental points are the values

$$S_F = \frac{2\pi e}{c\hbar} \frac{1}{\Delta(1/H)}$$

(where  $e$  is the electron charge,  $c$  the light velocity), while the curves are the extremal sections of the quasiellipsoidal model of the Bi Fermi surface. The mass coefficients are taken from the literature.<sup>12</sup>

(ii) When  $\vec{H}$  is parallel to the sample surface in the trigonal-bisector plane a sharp reduction of the QEO amplitude is observed (Fig. 5), while the measured  $S_F$  values are smaller than the extremal ones (Fig. 6).

The condition  $\vec{H}$  parallel to the sample surface has been obtained by means of the tilt effect in the absorption of ultrasounds, evidenced simultaneously to the microwave-absorption measurements. It is well known that the absorption of ultrasounds is reduced when  $\vec{H}$  becomes orthogonal to the ultra-

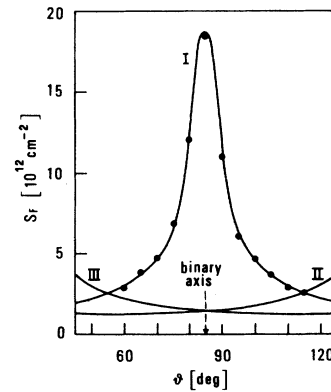


FIG. 3. Cross-sectional area  $S_F$  of the Fermi surface for  $\vec{H}$  rotating in the binary-bisector plane. Full points are experimental results, solid curves are the cross-sectional areas given by the literature (Ref. 11).

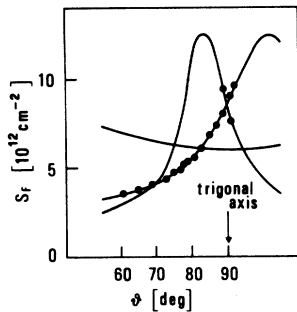


FIG. 4. As in Fig. 3. In this case  $\vec{H}$  is rotating in the trigonal-bisector plane.

sound wave vector  $\vec{q}$  as the quasimomentum  $k_H$  of the electrons, which can absorb ultrasounds, approaches  $k_H^F$ . In other words it is easy to show that  $k_H$  is a function of the angle  $\pi/2 - \alpha$  between  $\vec{H}$  and the ultrasound direction.

In Fig. 7 the ultrasound echo-pulse amplitude as a function of  $\alpha$  is reported at a fixed magnetic-field value: the maximum corresponds to the minimum absorption. By means of this method the alignment of  $\vec{H}$  with respect to the surface is given with an accuracy of  $0.1^\circ - 0.2^\circ$ . The angle for which the effect of Fig. 5 is observed is about  $12^\circ$  apart from the trigonal axis.

(iii) The QEO amplitude depends on the angle between  $\vec{H}$  and the surface normal. For angles smaller than  $65^\circ - 70^\circ$  the oscillation amplitude goes to zero.

(iv) The amplitude disappears for  $H$  larger (or for the resonance-order number  $n$  smaller) than a certain value (Figs. 1 and 2). At the same time, only QEO with large values of cross-sectional area  $S_F$  are measured: e.g., in Fig. 3, for  $\vec{H}$  lying in the binary-bisector plane, QEO are related to  $S_F$

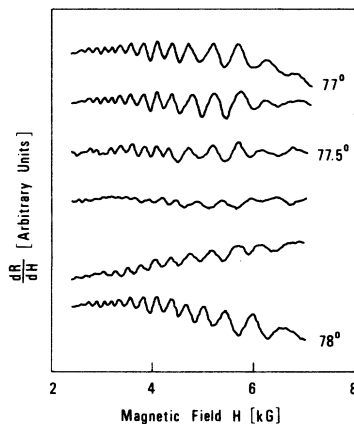


FIG. 5. Microwave absorption  $dR/dH$  vs  $H$  for various orientations of the magnetic field in the trigonal-bisector plane for  $\vec{H}$  nearly orthogonal to  $\vec{q}$ .

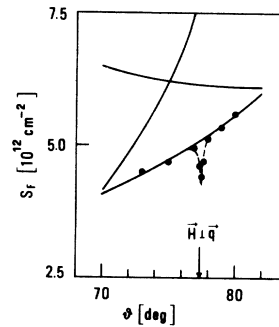


FIG. 6. Enlargement of central part of Fig. 4. Here the  $S_F$  values of Fig. 5 are reported.

values larger than  $2 \times 10^{12} \text{ cm}^{-2}$  (full points on curve I) while smaller areas are simultaneously present in Bi (curves II and III). These experimental features must particularly be underlined because they are peculiar of QEO.

(v) The behavior of  $dR/dH$  vs  $H$ , for certain directions of  $\vec{H}$ , is very complex, due, presumably, to the superimposition of oscillations of different carrier pockets. The measures presented in Figs. 3 and 4 are related to oscillations whose periods are easily found. The analysis of superimposed periods is more difficult than the corresponding one in giant ultrasound absorption, because, in the present case, the derivative  $dR/dH$  of the absorption signal is measured and resonances are not present for all the values of the order number  $n$  [see (iv)].

(vi) QEO are not present if the size  $l$  of the sample along the microwave propagation direction is smaller than 4.5 mm. Samples with  $l$  between 4.0 and 5.5 mm were used. For  $l < 4.7$  mm, QEO related to electrons were not observed. For  $l = 4.7$  mm QEO related to the holes are observed. For  $\vec{H}$  nearly parallel to the sample surface Alfvén oscillations superimposed to the hole QEO are present (Fig. 8), as already seen for the electrons by Dinger and Lawson.<sup>7</sup> For  $l < 4.5$  mm only oscillations of Alfvén type are present (Fig. 9). For this case the measured periods are related to the sam-

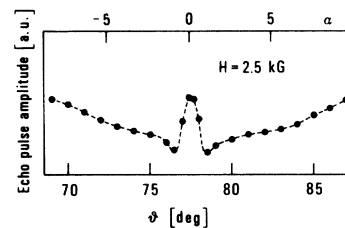


FIG. 7. Echo-pulse amplitude as a function of the angle  $\pi/2 - \alpha$  between the normal to the sample surface and the magnetic field direction. The magnetic field strength is 2.5 kG.

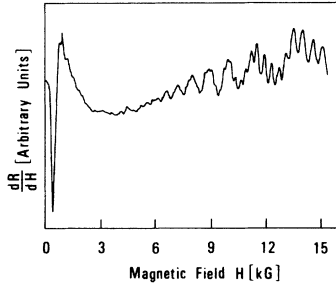


FIG. 8. Hole quantum oscillations with superimposed Alfvén oscillations when the sample size  $l$  along the microwave propagation direction is 4.7 mm.

ple size  $l$  and the coefficient<sup>13</sup>  $f(nm_e^* + pm_h^*)$  by

$$\Delta\left(\frac{1}{H}\right) = \frac{\lambda_0}{2l} (4\pi m_0 c^2)^{-1/2} f(nm_e^* + pm_h^*)^{-1/2},$$

where  $n$  and  $p$  are the carrier concentrations,  $m_e^*$  and  $m_h^*$  are the effective masses of the electrons and holes, respectively  $\lambda_0$  is the wavelength of the microwave in vacuum, and  $l$  is the sample size along the wave vector  $\vec{q}$ . The experimental values of  $f(nm_e^* + pm_h^*)$  are in agreement with those of Isaacson and Williams.<sup>13</sup>

(vii) In order to support the experimental results described in (iv), simultaneous absorption measurements of ultrasounds and microwaves by means of the experimental setup reported in Ref. 11 with  $\vec{H}$  rotating in the binary-bisector plane have been carried out. In Fig. 10 the behavior of the two absorptions is displayed for  $\vec{H}$  along the binary axis. As can be seen, for microwaves the oscillations are present at higher fields (large cross-sectional area) while for ultrasounds the resonances are present for lower fields (small cross-sectional area).

#### IV. DISCUSSION OF EXPERIMENTAL RESULTS

All of the experimental results reported in Sec. III allow us to say that the QEO are types of oscillations different from those found up to now. In particular, in Ref. 8 the authors themselves stress that there is no dependence of the amplitude of the oscillations on the angle between  $\vec{H}$  and the normal

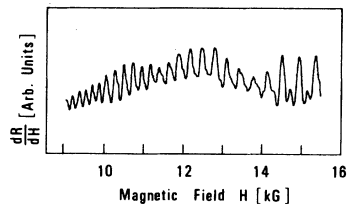


FIG. 9. Alfvén oscillations for the sample size  $l < 4.5$  mm.

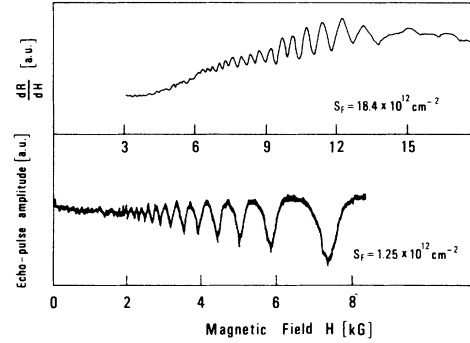


FIG. 10. Simultaneous measurements of microwave absorption (upper curve) and ultrasound absorption (lower curve) for  $\vec{H}$  along the binary axis.

to the surface, which constitutes a critical difference from our experimental results reported in point iii). The quantum nature of the QEO is their main feature, meaning that the resonances are associated to the quantization of the carrier energy levels in a magnetic field (Landau quantization). To show this, two results must be recalled:

(1) The periods  $\Delta(1/H)$  are directly related to the cross-sectional areas of the Fermi surface, full points in Figs. 3 and 4. In these figures the solid lines refer to the extremal cross-sectional areas calculated with a quasiellipsoidal model of the Fermi surface of bismuth. This model, as is well known, allows one to explain most of the experimental results (de Haas-van Alphen, ultrasound giant oscillations, etc.).

(2) When  $\vec{H}$  is nearly parallel to the sample surface, therefore nearly orthogonal to the wave vector  $\vec{q}$  of the electromagnetic wave, the QEO amplitude is reduced and the cross-sectional areas are not extremal.

In the same way as for the ultrasound quantum oscillations, the previous effects can be explained by means of the energy and momentum conservation laws, applied to the absorption of a photon by an electron. As a consequence of this assumption, when  $\vec{H} \perp \vec{q}$ , the oscillations must disappear. A total disappearance has not been observed. This may be due to an insufficient angular resolution, as can be shown by the following argument.

Let us calculate the electron quasimomentum  $k_H$  along the  $\vec{H}$  direction as a function of the angle  $\pi/2 - \alpha$  between  $\vec{H}$  and  $\vec{q}$  [here,  $\pi/2 - \alpha$  is the angle between the magnetic-field direction and the electromagnetic wave vector; it is the same, in our experimental arrangement, as the one defined in point (ii) of Sec. III]; when  $k_H$  becomes larger than  $k_H^F$  ( $k_H^F$  is the quasimomentum at the Fermi surface) photon absorption is forbidden. The conservation laws in the photon absorption give

$$\frac{\hbar^2 q_H k_H}{2m} = \hbar\omega, \quad (1)$$

where  $q_H = q \sin\alpha$ ,  $\hbar\omega$  is the photon energy, and  $m$  is the electron mass. Equation (1) is valid under the following conditions: A quadratic dispersion law for the carriers,  $\Omega_c \gg \omega$  (where  $\Omega_c = eH/mc$  is the cyclotron frequency) and  $q_H \ll k_H$ . These conditions imply that transitions between Landau levels are forbidden ( $\Delta n = 0$ ). Since  $k_H$  must be larger than  $k_H^F$ , one obtains

$$\sin\alpha \leq \frac{m\omega}{\hbar q k_H^F}.$$

Let us find  $\vec{q}$  when  $\vec{H}$  is nearly parallel to the surface, under the anomalous skin-effect condition. Using the "ineffectiveness" concept, one obtains

$$q = \left( \frac{4\pi\omega\sigma}{c^2 l} \right)^{1/3} \cos \frac{\pi}{3},$$

where  $\sigma/l = ne^2\tau/ml \cong ne^2/m\langle v \rangle$ ,  $\sigma$  is the static conductivity,  $l$  the mean free path, and  $\langle v \rangle$  is the mean velocity of the carriers. Then

$$\sin\alpha \leq \frac{m\omega}{\hbar k_H^F} \left( \frac{c^2 m \langle v \rangle}{4\pi\omega n e^2} \right)^{1/3} \left( \cos \frac{\pi}{3} \right)^{-1}.$$

For Bi ( $\langle v \rangle \cong 10^6$  cm/sec,  $n = 10^{18}$  cm $^{-3}$ ,  $\omega = 2\pi \times 24 \times 10^9$  sec $^{-1}$ ,  $k_H^F \cong 5 \times 10^5$  cm $^{-1}$ ), one obtains  $\sin\alpha \cong \alpha \leq 10^{-2}$  deg. Therefore, the QEO must disappear for  $\vec{H}$  parallel to the sample surface within  $10^{-2}$  deg. We have found a sharp reduction of both the resonance amplitude and the cross-sectional area in a  $0.5^\circ$  range as is shown in Fig. 6. Both the planarity of the sample surface and our experimental angular resolution were poorer than  $0.1^\circ$ .

As a consequence of all the previous arguments we can say that the quantum origin of the QEO is well stated. Then the resonance minima are due to the Landau levels crossing the Fermi level and the order number  $n$  in Fig. 2 must be considered as the Landau quantum number. Once stated (the nature of the QEO), let us consider in the following the characteristic aspects of these oscillations.

The most important feature is the lack of resonances for some values of  $n$ . In fact the disappearance of oscillations, pointed out in (iv), beyond a certain value of the magnetic field, means that resonances are not present below a Landau quantum number  $n_{\min}$ . Note that in the quantum effects known up to now (de Haas-van Alphen, giant quantum oscillations, etc.), the resonance amplitude grows up continuously with increasing magnetic field (with decreasing Landau quantum number), because the electron density of the quantum levels increases with the magnetic field. For each magnetic-field direction, where QEO are present, it is possible to measure  $n_{\min}$  and  $S_F$ . These values

are reported in Fig. 11 (full points). In the same figure the solid line represents the logarithmic fit

$$n_{\min} = b \ln \left( \frac{S_F}{1.5S_0} \right),$$

with the best-fit parameters  $b = 6.35$ ,  $S_0 = 1 \times 10^{12}$  cm $^{-2}$ . The extrapolated value of  $S_F$  for  $n_{\min} = 0$  is  $S_{F0} = 1.5 \times 10^{12}$  cm $^{-2}$ . QEO with cross-sectional areas below  $S_{F0}$  were not measured, though, in bismuth, Fermi-surface sections with  $S_F < S_{F0}$  are present for many magnetic-field directions.

This is another peculiar aspect, because, as it is well known, small cross-sectional areas are more easily detected within the same magnetic-field range in the de Haas-van Alphen or in giant quantum oscillations. This feature is well stressed in Fig. 10, where the small cross-sectional area  $S_F = 1.25 \times 10^{12}$  cm $^{-2}$  is detected only by means of giant quantum oscillations of ultrasounds. We can summarize these points in the following way: Resonances are present for points  $(n, S_F/S_0)$  inside the dashed region of Fig. 11. The interpretation of these effects can be found either in some peculiarity of the carrier dispersion law of Bi or in the nature of the electromagnetic waves supporting the QEO.

A possible explanation, related to the dispersion law, suggested by the large values of the measured cross-sectional areas, and by the logarithmic behavior of the curve in Fig. 11, can be the following: The transparency of the classically forbidden zone between different pockets of carriers increases with magnetic-field intensity. When the carriers are no more localized in a well-defined pocket of the Brillouin zone, the cross-sectional areas of the Fermi surface become very large and the related oscillations are outside of our experimental magnetic-field range.

Following this line of thought, a rough calculation can be carried out assuming that in the classically

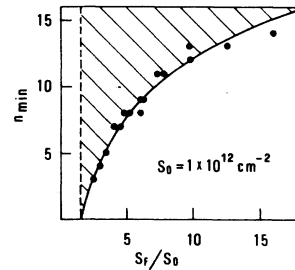


FIG. 11. Landau quantum number  $n_{\min}$  as a function of the cross-sectional area  $S_F$  (full points).  $n_{\min}$  is the last level for which resonances are measured (see Fig. 2). The solid line represents a logarithmic fit. QEO resonances are present only for the points  $(n, S_F/S_0)$  inside the dashed region.

forbidden region between two pockets a cylinder-parabolic differential equation holds.<sup>14</sup> The energy eigenvalues are given by the relation

$$\cot\left(\frac{S_1}{2\lambda_0} + v_2\right) \cot\left(\frac{S_2}{2\lambda_0} + v_2\right) = \exp(-2\pi |a_1|),$$

where

$$a_1 = \frac{E - \epsilon_0 - \beta_3 k_x^2 + (\beta_3^2/\beta_2) k_x^2}{2\lambda_0 \sqrt{-\beta_1 \beta_2}}, \quad \lambda_0 = \frac{eH}{\hbar c},$$

$S_1$  and  $S_2$  are the cross-sectional areas of the two pockets, and the  $\beta_i$ 's are functions of the effective-mass coefficients. When  $a_1 \rightarrow \infty$ , then  $v_2 = 0$ ,  $\exp(-2\pi |a_1|) = 0$ , and the usual quantization laws are obtained:

$$\frac{S_1}{2\lambda_0} = (2n_1 + 1) \frac{\pi}{2}, \quad \frac{S_2}{2\lambda_0} = (2n_2 + 1) \frac{\pi}{2},$$

while, for  $a_1 \rightarrow 0$  ( $H \rightarrow \infty$ ), one obtains

$$\cot\left(\frac{S_1}{2\lambda_2}\right) \cot\left(\frac{S_2}{2\lambda_0}\right) = 1$$

and the quantization is

$$\frac{S_1 + S_2}{2\lambda_0} = (2n + 1) \frac{\pi}{2}.$$

In this case oscillations related to added areas must be found. The value  $|a_1|$  is given by

$$|a_1| = \frac{d^2}{4} \left(\frac{\beta_1}{\beta_2}\right)^{1/2} \frac{c\hbar}{eH},$$

where  $d$  is the linear size of the classically forbidden region. In the case of Bi, taken  $d = 10^8$  cm<sup>-1</sup>,  $(\pi/2) |a_1| \cong (\beta_1/\beta_2)^{1/2} (10^6/H)$ . Therefore, for  $H < 2 \times 10^4$  G (in this model and with such a rough estimate), no hybridization can exist.

On the other hand, a lack of resonance below  $n_{\min}$  has not been found in ultrasound absorption. The difference between microwave and ultrasound absorption lies in the field-carrier interaction potential and in the fact that the photon energy is about  $10^2$  times bigger than the phonon one. A possible explanation, along the line sketched above, might perhaps be found if these different conditions were taken into account together with the peculiarities of electromagnetic-wave propagation in a metal.

If the nature of the electromagnetic waves supporting the quantum oscillations is considered, one meets with a problem very hard to face. A quantum theory for the propagation of electromagnetic waves in metals with a magnetic field present has been formulated by many authors.<sup>15-17</sup>

Reference 15 gives a theory of the absorption assuming a quadratic dispersion law for the carriers: It is found, in the limit  $\hbar\omega \ll \hbar\Omega \sim \epsilon_F$ , that the absorption is of the de Haas-Van Alphen type. Owing to the lack of experimental results, the theories

reported in Refs. 16 and 17 are not specific and are difficult to use for looking into the actual physical situations.

The point is that together with the absorption, the wave dispersion is also affected by the quantization induced by the magnetic field. We have pointed out above that the QEO are analogs of the ultrasound giant oscillations,<sup>18</sup> but the main difference lies in the fact that while the ultrasounds have a very simple ( $\omega = qv_s$ , where  $v_s$  is the sound velocity) dispersion law, in the case of the microwaves  $\omega(q)$  may be a very complicated function. Following the paper of Kaner and Skobov<sup>19</sup> we are able to give a model that explains the main features of the QEO.

Let us assume that (a) the carriers obey an ellipsoidal dispersion law, (b) the temperature is 0°K, and (c)  $\omega\tau \gg 1$ ; under these hypotheses and in the semiclassical limit Kaner and Skobov give a theory that allows the calculation of the dispersion law  $\omega(q) = \omega$  [or  $u(\omega) = u$ , where  $u = \omega/q$  is the wave-phase velocity]. Their conclusions give the dispersion law as an implicit equation:

$$1 \mp \frac{\omega}{\omega_r} - \left(\frac{u}{v_a}\right)^2 = \gamma G(u), \quad (2)$$

where

$$G(u) = \sum_{n=0}^N \zeta_n \left[ \left(1 - \frac{u^2}{v_n^2}\right)^{-1} - 1 \right],$$

$$\zeta_n = \left(\frac{n}{N}\right)^2 [N(N + \Delta - n)]^{-1/2}.$$

$N$  is the last occupied Landau level,  $\Delta$  is defined by  $(N + \Delta)\hbar\Omega = \epsilon_F$ ,  $v_n = [2(\epsilon_F - n\hbar\Omega)/m]^{1/2}$ ,  $v_a$  is the Alfvén velocity which is proportional to  $H$ ,  $\omega_r \sim \Omega(v_a/v_F)^2$  is proportional to  $H^3$ , and  $\gamma$  is a parameter depending on  $H$  and  $\epsilon_F$ , which is much larger than 1 when  $H < 10^6$  G.

Equation (2) is very difficult to solve, but a graphical analysis can be given in order to develop a qualitative model, following the lines suggested by Fig. 1 in Ref. 19. For a given  $H$  the real values of  $u(\omega)$  are the intersections (see Fig. 12) of  $\gamma G(u)$  with the parabolas  $1 \pm \omega/\omega_r - (u/v_a)^2$ . The curve  $G(u)$  presents an infinite discontinuity when  $u$  equals  $v_n$ . Let us consider the parabola with the minus sign, which is more suitable for our purposes, and let us direct our attention to the absorption. Under the above-stated conditions, Landau damping does not allow the propagation of electromagnetic waves when

$$|u - v_n| < \frac{\hbar q}{2m_*} = \frac{\hbar\omega}{2um_*}. \quad (3)$$

Equation (3) is the energy and momentum conservation law in the wave-vector  $\vec{q}$  photon absorption and can be represented in Fig. 12 by the rectangles centered on  $u = v_n$ . Then, the waves whose

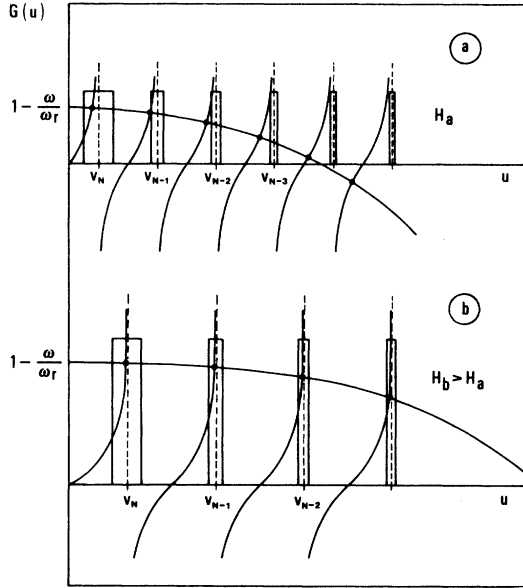


FIG. 12. Graphical solution of Eq. (2). Dots represent the real solutions for  $u(\omega)$ . Cases (a) and (b) refer to different values of the magnetic field. In case (a),  $H_a < H_b$ , resonances are possible; in case (b) no resonance exists on increasing the magnetic-field intensity.

point solutions fall into the rectangles are damped.

To understand our model three circumstances must be considered:

- (i) the width of the rectangles grows as  $u$  goes to zero;
- (ii)  $\omega_r$  increases as  $H^3$ ;
- (iii)  $v_a$ , which gives the intersection of the parabola with the  $u$  axis, increases with  $H$ .

The carrier velocity  $v_N$  of the  $N$ th Landau level at  $\epsilon = \epsilon_F$  goes to zero when  $H$  increases because the Landau level leaves the Fermi surface. Then, the combined effects of the spreading of the rectangle base and of the zeroing of  $v_N$  make the first point solution fall into the first rectangle, giving place to a resonant absorption, while the other wave solutions continue to propagate [Fig. 12(a)]. As a consequence the measured cross sections of the Fermi surface are essentially the extremal ones ( $p_x = 0$ ) as our measurements show. As the magnetic field increases far beyond the values considered in drawing Fig. 12(a),  $\omega_r$  and  $v_a$  increase

and the parabola tends to flatten and to rise; in these conditions all the intersections fall into the rectangles and thus represent damped waves. That is to say, no other resonances are possible as a function of  $H$  [Fig. 12(b)].

## V. CONCLUSIONS

In this paper we have reported the first observation of microwave absorption oscillations related to the quantization of Landau levels in a magnetic field in the collisionless-damping regime, i.e., when the conservation laws are fulfilled in the interaction of an electron with a Bose excitation. The main features of the effect are as follows:

(i) The periods  $\Delta(1/H)$  are directly related to the cross-sectional areas of the Fermi surface.

(ii) The oscillations are present only if the size of the sample along the wave propagation direction is larger than 0.5 cm; below this value Alfvén oscillations are observed.

(iii) Resonances are not seen for every crossing of Landau levels through the Fermi level; only levels corresponding to points which lie in the dashed region of Fig. 11 can absorb.

(iv) The resonance amplitudes are maxima when the  $\vec{H}$  direction is nearly parallel to the sample surface.

These types of oscillations have been predicted<sup>16,17</sup> following the giant quantum oscillations in ultrasound absorption, and a  $\Delta(1/H)$  period connected to the cross-sectional areas has been calculated. This is in agreement with the first feature listed above.

On the other hand, the ellipsoidal-nonparabolic, (ENP) model<sup>20</sup> is able to give the measured values of the cross sections as functions of the angle between  $H$  and the crystallographic directions. As is well known,<sup>10,21</sup> in order to detect deviations from the ENP one must measure the cyclotron masses and compare them with the cross-sectional areas. We have attempted an explanation of the other features by means of a first-approximation calculation, assuming a tunneling between different pockets of carriers, but the results are not consistent with the parameters for bismuth. A more suitable model has been given which takes into account not only the absorption, but also wave dispersion when magnetic quantization is present.

- <sup>1</sup>E. A. Kaner and V. G. Skobov, *Adv. Phys.* 17, 605 (1968).
- <sup>2</sup>M. Maltz and M. S. Dresselhaus, *Phys. Rev. B* 2, 2877 (1970).
- <sup>3</sup>U. Strom, A. Kamgar, and J. F. Koch, *Phys. Rev. B* 7, 2435 (1973).
- <sup>4</sup>D. S. Mc Lachlan, *Phys. Rev.* 147, 368 (1966).
- <sup>5</sup>R. T. Isaacson and G. A. Williams, *Phys. Rev. Lett.* 22, 26 (1969).
- <sup>6</sup>H. Kawamura, S. Nagata, T. Nakama, and S. Takano, *Phys. Lett.* 15, 111 (1965).
- <sup>7</sup>R. J. Dinger and A. W. Lawson, *Phys. Rev. B* 7, 5215 (1973).
- <sup>8</sup>F. W. Spong and A. F. Kip, *Phys. Rev.* 137A, 431 (1965).
- <sup>9</sup>V. Ya. Demikhovskii and A. P. Protogenov, *Usp. Fiz. Nauk* 118, 101 (1976) [*Sov. Phys. Usp.* 19, 53 (1976)].
- <sup>10</sup>M. Giura, R. Marcon, and P. Marietti, *Solid State Commun.* 21, 887 (1977).
- <sup>11</sup>M. Giura, R. Marcon, and P. Marietti, *J. Low Temp. Phys.* 29, 397 (1977).
- <sup>12</sup>T. Sakai, Y. Matsumoto, and S. Mase, *J. Phys. Soc. Jpn.* 27, 862 (1969).
- <sup>13</sup>R. T. Isaacson and G. A. Williams, *Phys. Rev.* 177, 738 (1969).
- <sup>14</sup>M. Giura, R. Marcon, and P. Marietti, *Nuovo Cimento* 29B, 49 (1975).
- <sup>15</sup>D. C. Mattis and G. Dresselhaus, *Phys. Rev.* 111, 403 (1958).
- <sup>16</sup>M. I. Azbel, *Zh. Eksp. Teor. Fiz.* 61, 1245 (1971) [*Sov. Phys.—JETP* 34, 669 (1958)]; 61, 1506 (1971) [34, 801 (1958)].
- <sup>17</sup>V. G. Skobov and E. A. Kaner *Zh. Eksp. Teor. Fiz.* 46, 1809 (1964) [*Sov. Phys.—JETP* 19, 1219 (1964)].
- <sup>18</sup>V. L. Gurevich, V. G. Skobov, and Yu. A. Firsov, *Zh. Eksp. Teor. Fiz.* 40, 786 (1961) [*Sov. Phys.—JETP* 13, 552 (1961)].
- <sup>19</sup>E. A. Kaner and V. G. Skobov, *Fiz. Tekh. Poluprovodn.* 1, 1367 (1967) [*Sov. Phys. Semicond.* 1, 1138 (1967)].
- <sup>20</sup>B. Lax, J. G. Mavroides, H. J. Zeiger, and R. J. Keyes, *Phys. Rev. Lett.* 5, 241 (1960).
- <sup>21</sup>J. W. McClure, *J. Low Temp. Phys.* 25, 527 (1976).